minerals

MDPI

Article

Deciphering Alterations of Rodent Bones through In Vitro Digestion: An Avenue to Understand Pre-Diagenetic Agents?

Christiane Denys [1,*], Denné N. Reed [2] and Yannicke Dauphin [1,3]

[1] UMR 7205 CNRS-MNHN-EPHE-SU UA, ISYEB (Institut de Systématique et Evolution de la Biodiversité), Museum National d'Histoire Naturelle, 57 rue Cuvier, 75005 Paris, France
[2] Department of Anthropology, University of Texas, Austin, TX 78712, USA
[3] Department of Biomaterials, Max-Planck Institute of Colloids and Interfaces, 14476 Potsdam, Germany
* Correspondence: christiane.denys@mnhn.fr

Abstract: Recent taphonomic studies have shown that avian predators such as owls are responsible for most small-mammal fossil accumulations, and that predators cause bone loss and breakage as well as modification to the surface of bones that are preserved. However, the specific physiochemical alterations and the alterations of bone microstructures that predators induce remain poorly understood. In order to better separate and characterize the effects of bone digestion by owls, we performed an experimental study to simulate digestion by a predator. We put fresh rodent long bones into various solutions to simulate the digestive effects of predators. We first tested an acid solution, followed by other solutions containing key enzymes such as trypsin, lipase, and trypsin + lipase. Next, we compared the results of the simulated digestion experiments with partly digested long bones recovered from *Tyto alba* and *Bubo bubo* pellets. We observed that acid action alone did not reproduce the modifications observed on bones from owl pellets, while the enzymatic activity (notably trypsin and trypsin + lipase) produced modifications most similar to those observed on the bones from the owl pellets. These results open a promising field of future experimentation to better understand the early diagenetic modification induced in small mammal bones by digestion, which can improve our ability to recognize the role of nocturnal predators in fossil accumulations.

Keywords: bone modifications; rodents; birds of preys; experiments; taphonomy

Citation: Denys, C.; Reed, D.N.; Dauphin, Y. Deciphering Alterations of Rodent Bones through In Vitro Digestion: An Avenue to Understand Pre-Diagenetic Agents? *Minerals* **2023**, *13*, 124. https://doi.org/10.3390/min13010124

Academic Editors: Alejandro B. Rodriguez-Navarro and Pieter Bertier

Received: 1 November 2022
Revised: 2 January 2023
Accepted: 8 January 2023
Published: 14 January 2023

1. Introduction

When introducing taphonomy as a new branch of palaeontology, Efremov [1] distinguished neotaphonomy as the study of the processes of fossilization affecting the modern accumulations before the burial phase. Among the different processes responsible for bone accumulations, predation is important, especially for microvertebrates [2]. Microvertebrates are often consumed whole, and the bones are subject to pre-burial mechanical and chemical modification as they pass through the digestive tract of the predator (Figure S1) [3]. These modifications include bone surface abrasion, bone loss, and fragmentation. Pre-burial alterations may in turn affect surface modifications occurring during the deposition and fossilization processes [2,4–7]. Among small vertebrates, rodents represent the bulk of the accumulations and have a recognized value in palaeoenvironmental reconstructions as well as indicators of fossil site formation processes. Most reconstructions (palaeoclimate, palaeobiodiversity, etc.) are based on a comparison between modern and ancient pellet contents from avian predators. The relative abundance of bones and teeth as well as the intensity and abundance of surface marks, fragmentation, and loss of bones may be used to identify the predator responsible for the original accumulation [7–13]. Unfortunately, such analyses may be biased as a result of the diet specificity of the predator, the existence of an extinct predator whose diet is unknown, or the absence of pellet reference material from a region [14–16].

Despite the expansion of literature using pellet contents in palaeoecological studies, there is still a paucity of data regarding histological and biochemical modifications related to digestion by owls. Moreover, some experimental data show that it may be difficult to separate abrasion from digestion features on bone surfaces [17]. Additionally, bone surface modification resulting from weathering, trampling, or from soil and sediment interaction (compaction, concretions, etc.) may obscure digestion traces [7,18].

Separating bone surface marks caused by digestion from those due to burial is a necessary step in the reconstruction of the origin and history of small mammal fossil accumulations. A detailed discussion of taphonomic studies is beyond the scope of this paper, but most studies rely on fragmentation and frequency of skeletal elements to identify predators [8–13,19–22], sometimes at a microscopic level [23]. Usually, fur and feathers are present in pellets, but not studied [19]. An alternate method is to simulate in vitro digestion using enzymes known to be present in the digestive tract of birds or to use pellets from known predators [24,25]. Despite a few attempts to better understand avian digestion processes, illustrations of bone microstructure modification due to digestion remain scarce.

Thus, in the present work, we first study the effects of acidic and enzymatic in vitro hydrolyses on the surface of rodent bones to unravel the respective role of the components of the raptor gastric juices. Then, we compare these alterations with those observed on long bones extracted from the pellets of two owl species, *Bubo bubo* and *Tyto alba*, commonly implicated as the source of fossil assemblages [4–6,8].

2. Materials and Methods

Rodent bones of wild animals were used for these experiments. The selected owl species ingest their prey whole (including hair and bones) and to replicate this we preserved most of the soft tissue (muscle, organs, etc.) but elected to remove most of the fur and skin to avoid any preliminary chemical and bacterial attacks before the acidic and enzymatic treatments. Experimentations were then performed on fresh bones without more preparation. This means that the selected bone retained the original meat, fat, tendons, nerves, etc. Acids and enzymes were used separately and in combination to investigate their individual roles in the digestion. Figure S2 shows the selected bones in the rodent skeleton and Figure S3 shows bone surfaces before the chemical treatments.

2.1. Material

2.1.1. Fresh Specimens

Three fresh wood mice (*Apodemus sylvaticus)* from France were used for these experiments. A juvenile and an adult female were found dead in a garden in Yvelines (France) and preserved intact in a freezer. An adult pregnant female was captured by a domestic cat in a garden from Vienne (France) and kept in a deep freeze. A juvenile mouse *(Mus musculus)* from Paris (MNHN—Jardin des Plantes) was used after being kept in a deep freeze.

Samples were thawed for one hour and the anterior and posterior legs (including skin, muscles, and long bones) were removed by scissors and tweezers and put into an Eppendorf tube and kept in the fridge until their treatments. The skulls of these specimens were used to verify the taxonomic identification and are housed in the Mammals collection at the MNHN.

2.1.2. Pellet Specimens

Bubo bubo pellets were collected in Southwest France (Alzon village, Lot) by L. Joubert in a nest and under rest places. The rodent *Apodemus sylvaticus* was the dominant prey species in this assemblage. A taphonomic analysis [21,22] revealed that femora were the best-preserved element, followed by mandibles and tibia. A total of 55.6% of femora showed surface modifications consistent with digestion, and 100% of humerus showed light to moderate grades of digestion. These results fit well with previous studies conducted on the taphonomy of this predator [26–29] (Table S1). *Tyto alba* pellets were collected by L. Granjon close to Chott Boul along the Atlantic coast of Mauritania in an abandoned

nest [26]. Samples were deposited in the collections of the Museum National d'Histoire naturelle under catalogue numbers CG-MNHN-ZM-2020-578 and 2020-576.

2.1.3. Enzymes Buffers

Trypsin: from hog pancreas, Fluka.
Lipase: from Candida rugosa, Sigma.
TRIS: 2-amino-2-hydroxyméthylpropane-1,3-diol, Sigma.

2.2. Methods

2.2.1. Bone Preparation

Fresh rodents were dissected using scalpels and tweezers. We avoided chemical methods or heating during removal of the soft tissues. These specimens were cleaned using a solution of Milli-Q water and a few drops of a commercial detergent at room temperature for 17 h 30 min under moderate agitation to mollify the residual flesh. They were given an ultrasonic treatment for 4 min to remove residual flesh, then rinsed in water with an ultrasonic treatment for 2 min, and air dried. Using this protocol, a maximum of flesh and muscle was removed without marking the surface of the bones. After this treatment, we noticed that the bones were still covered by soft tissue (skin, hair, and muscle), indicating that no dissolution occurred during the cleaning phases despite the relatively long water immersion (Figure S3).

Owl pellet preparation: long bones of rodents were extracted from the pellets manually using tweezers and no water was employed. No supplementary treatment was performed to sort the bones.

2.2.2. Observations

The first observations of digestion grades were conducted using a stereomicroscope. Then, fresh and etched samples were observed using an FEI PHENOM PROX microscope in back-scattered electron (BSE) mode; images were obtained without coating, at 15 kV accelerating voltage. BSE consists of high-energy electrons reflected or back-scattered out of the specimen. As a result, mineral-enriched zones are brighter than those enriched in organic components [30]. Qualitative electron dispersive spectrometry (EDS) spectra were used to observe the chemical changes. An FEI QUANTA FEG 600 (Max Planck Institute of Colloids and Interfaces, Potsdam, Germany) was used in both (BSE) and secondary electron (SE) modes in low vacuum, at 5 or 15 KeV accelerating voltage.

Owl pellet samples were observed using a SU 3500 scanning electron microscope (Hitachi, Paris, France) at 10 keV (Plateau technique de Microscopie Electronique et de Microanalyse (PtMEM) G. Toutirais) of the MNHN. These samples were gold-palladium coated.

2.2.3. Experimental Set Up of Acidic and Enzymatic Hydrolyses

For all experiments, samples were put in the etching solution for 9 h at 36–37 °C, under constant stirring. They were then rinsed with Milli-Q water and air dried at room temperature. Acid hydrolysis: HCl pH 1 and pH 2.43. Enzymatic hydrolyses: (a) trypsin (12,488 units/mg): 1 mg/mL and 5 mg/mL in TRIS buffer pH 7.5; (b) lipase (685 units/mg): 5 mg/mL in TRIS buffer pH 7.5; (c) a mixture of trypsin 5 mg/mL and lipase 5 mg/mL in TRIS buffer pH 7.5. For each experiment, bones were etched in 20 mL solutions.

3. Results

3.1. Unetched Bones

The main features of bone structure are described in Figure S4.

A *Mus musculus* femur cleaned with water and detergent is partly covered with residual flesh and periosteum (Figure 1A,B). When the organic tissues are destroyed, the resorbing surface shows the usual depressions and the haversian system (Figure 1C). Some hairs are still visible on the femur of the pregnant female *Apodemus* (Figure 1D), but the inner structure of the bone is locally apparent (Figure 1D,E). Lamellar bone is visible in

some fractures (Figure 1F). BSE images of a humerus epiphysis show that the organic tissues are not fully destroyed by the mild cleaning (Figure 1G). Removal of the soft tissues reveals the porosity of this part of the bone and the resorption patterns (Figure 1H). Larger magnifications show the haversian system (Figure 1I).

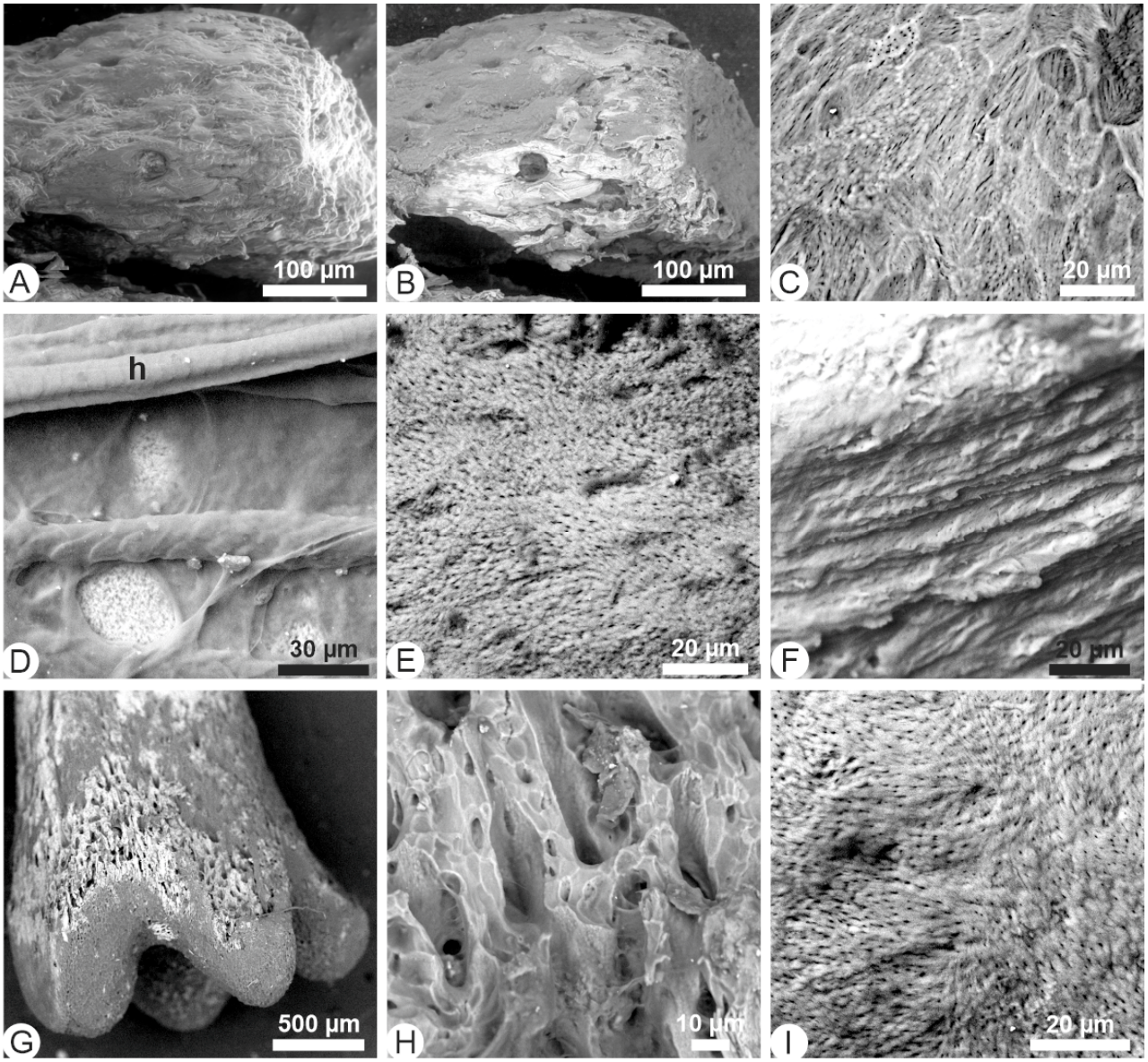

Figure 1. Fresh bone samples. A, B. *Mus musculus:* secondary electron (SE) SEM image (**A**) and back-scattered electron image (BSE) of the same zone (**B**); BSE image reveals the presence of organic tissues on the surface (in dark). (**C**). Resorbing surface and the haversian system femur. (**D**). Hairs on the same bone. (**E**). Inner structure of the bone. (**F**). Lamellar bone visible in some fractures; same bone. (**G**). Humeral epiphysis of *Apodemus*; BSE image shows the light region (mineral) and the dark zones (organics). (**H**). Porosity and resorption patterns. (**I**). Haversian system in a bone of *Apodemus*.

3.2. Acidic Hydrolyses

Hairs are still preserved on the scapula of *Apodemus* after the HCl pH 1 hydrolysis (Figure 2A). The haversian structure is hidden by flesh remains (Figure 2B–D). The bone is soft and flexible before it dries. Similar features are observed using a pH 2.43 HCl solution on a tibia of the same animal (Figure 2E–F). Muscular fibers are more or less dissociated (Figure 2F), and hairs are abundant in the articular zone (Figure 2G). Electron microprobe spectra of three different zones (Figure 2H) show that the bones are decalcified

(Figure 2I). Ca and P are absent or very weak, while S (linked to the organic matrix) is present. Both bones (tibia, scapula) were fully decalcified using HCl solutions. Only the organic components are preserved (hairs, flesh, and organic components of the bone itself).

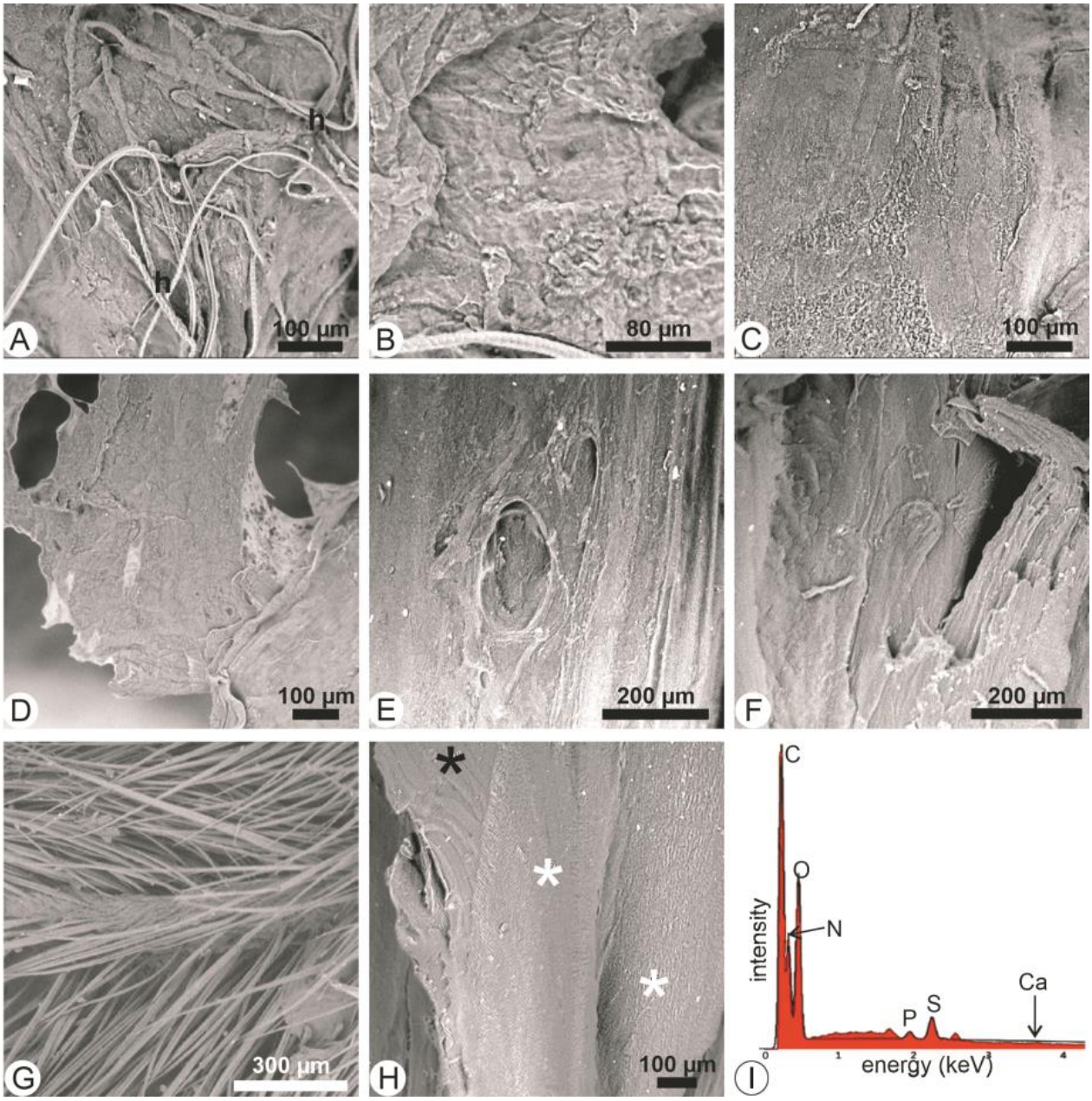

Figure 2. Acidic hydrolyses. (**A**). Hairs on the scapula (*Apodemus*); HCl pH 1. (**B**–**D**). Haversian structure hidden by flesh remains; HCl pH 1. (**E**–**F**). Tibia of the same sample showing similar features; HCl pH 2.43. (**G**). Hairs in the articular zone; HCl pH 2.43. (**H**). Localization of electron microprobe spectra: white stars. (**I**). Spectra showing the loss of Ca and P in acidic etched bones.

3.3. Trypsin Hydrolyses

The lamellar structure of the femur of *Apodemus* is displayed by the use of a dilute solution of trypsin (Figure 3A). BSE images of the surface of a femur (*Apodemus*) clearly show the contrast between the mineral (light grey) and the dark gray hairs and cells (Figure 3B,C). Resorbing bone depressions on the surface of the same femur are distinct (Figure 3D,E), and between these depressions, the haversian system is visible (Figure 3F).

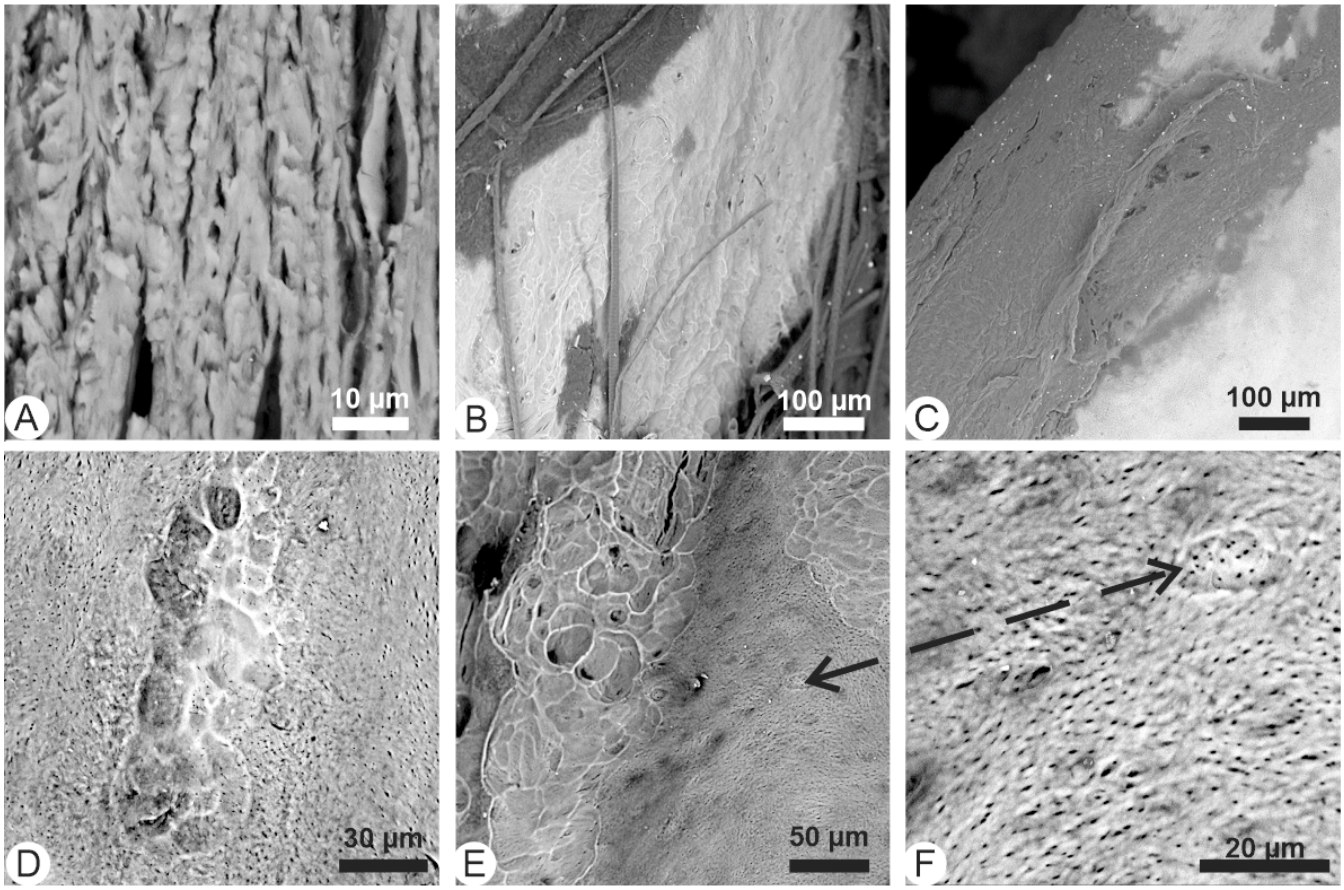

Figure 3. Trypsin hydrolyses (1 mg/mL). (**A**). Lamellar structure of the humerus *Apodemus*. (**B**). BSE image of the same sample showing some hairs on the surface. (**C**). Flesh remains on the surface of the same sample. (**D**,**E**). Resorbing bone is visible when the organic tissues are destroyed. (**F**). Arrows: detail of Figure 3E showing the Haversian system visible between the bone depressions of the same sample.

Comparing SE (Figure 4A) and BSE (Figure 4B) images of the humerus epiphysis of *Mus* confirms that trypsin is efficient at destroying flesh, but a few areas are still covered by the organic tissues despite a higher concentration of the enzyme. The condyle surface and the epiphysis of a tibia (*Apodemus*) are porous at low magnifications (Figure 4C–F). The surface shows wavy zones with cupules due to the bone resorption at the surface of the femur (*Apodemus*) and the haversian structure (Figure 4G). Electron microprobe spectra of the tibia show that P and Ca are present in the usual ratio (Figure 4H,I). Na, Mg, and S are also detected.

3.4. Lipase Hydrolyses

Soft tissues are only locally destroyed by the lipase, as shown by the comparison of the SE (Figure 5A) and BSE (Figure 5B) images of the extremity of a femur of *Apodemus*. The bottom of the porous cancellous structure is still rich in organic matrix (Figure 5C).

The small lacunae of the haversian structure are visible in clean zones of the scapula of *Apodemus* (Figure 5D,E). Nevertheless, the pattern is less distinct, and no cupule has been observed. Hairs are not etched (Figure 5F). A clean bone surface (without remains of muscle) is pale yellow, and the zones with flesh are brown when seen with an optical camera (Figure 5G). EDS spectra of a clean surface show that the sample is not decalcified (Figure 5H,I).

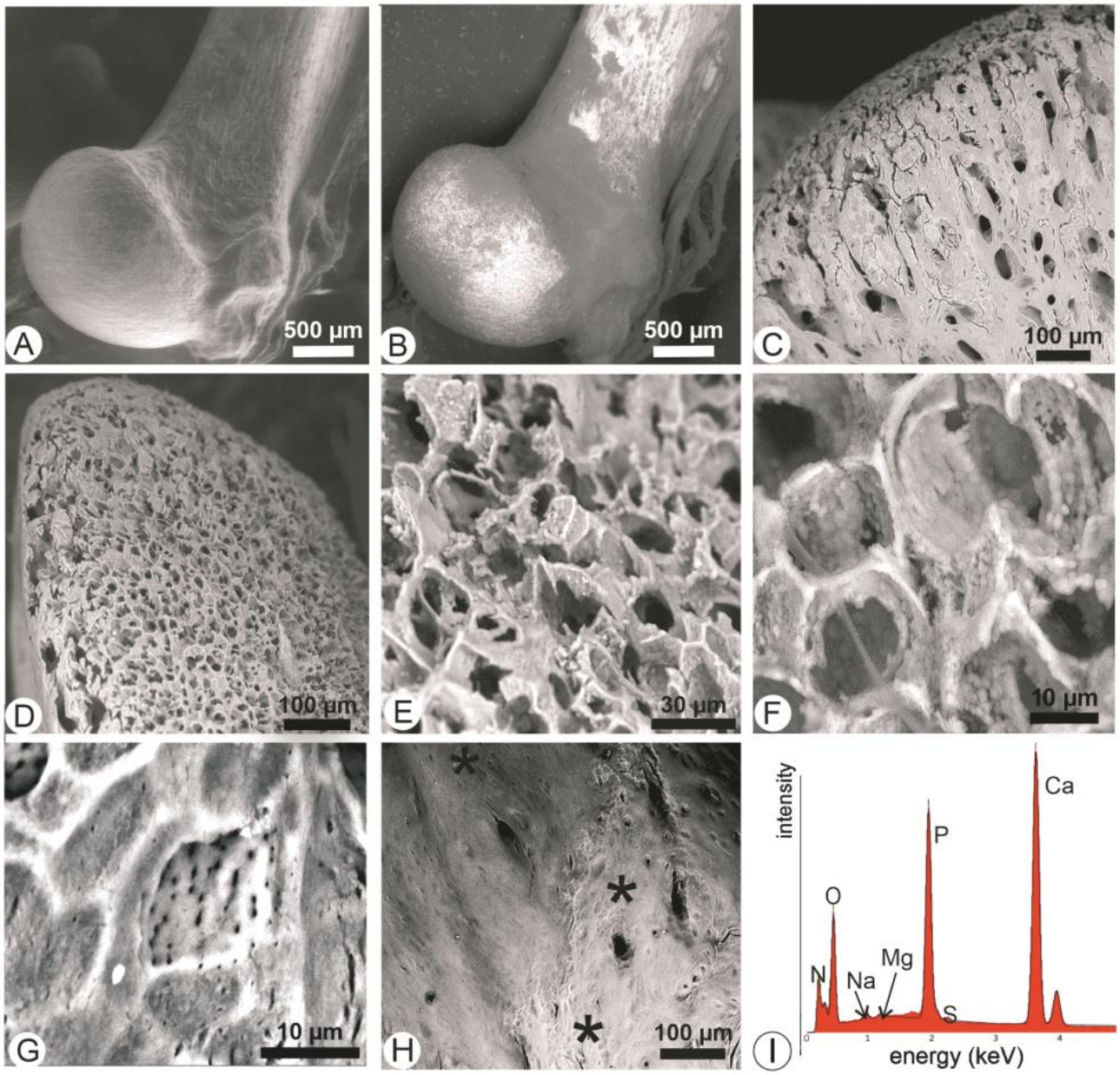

Figure 4. Trypsin hydrolyses (5 mg/mL). (**A**,**B**). Humeral epiphysis of *Mus*; A: SE image, B: BSE image. (**C**–**F**). Porosity of the condyle and epiphysis of a tibia (*Apodemus*). (**G**). Haversian system and wavy zones and cupules due to the bone resorption femur (*Apodemus*). (**H**) Localization of electron microprobe spectra: stars (**I**). Spectra show that P and Ca are present as well as Na, Mg and S.

3.5. Trypsin + Lipase Hydrolyses

Only a part of the organic tissues was removed by the mixed enzymatic solution, as shown by SE (Figure 6A) and BSE (Figure 6B) images of the epiphysis of a femur of *Apodemus*. The solution is more efficient on the outer part of a fractured tibia of *Apodemus* (Figure 6C). The BSE image displays the irregular etching of the solution on the epiphysis of a femur of *Apodemus* (Figure 6D). Small rounded granules are visible in the alveoles of the cancellous zone of a tibia (*Apodemus*) (Figure 6E,F). Bone resorption patterns clearly show the bone structure in the same sample (Figure 6G,H) and in the femur of *Mus musculus* (Figure 6G,I). No hair is visible.

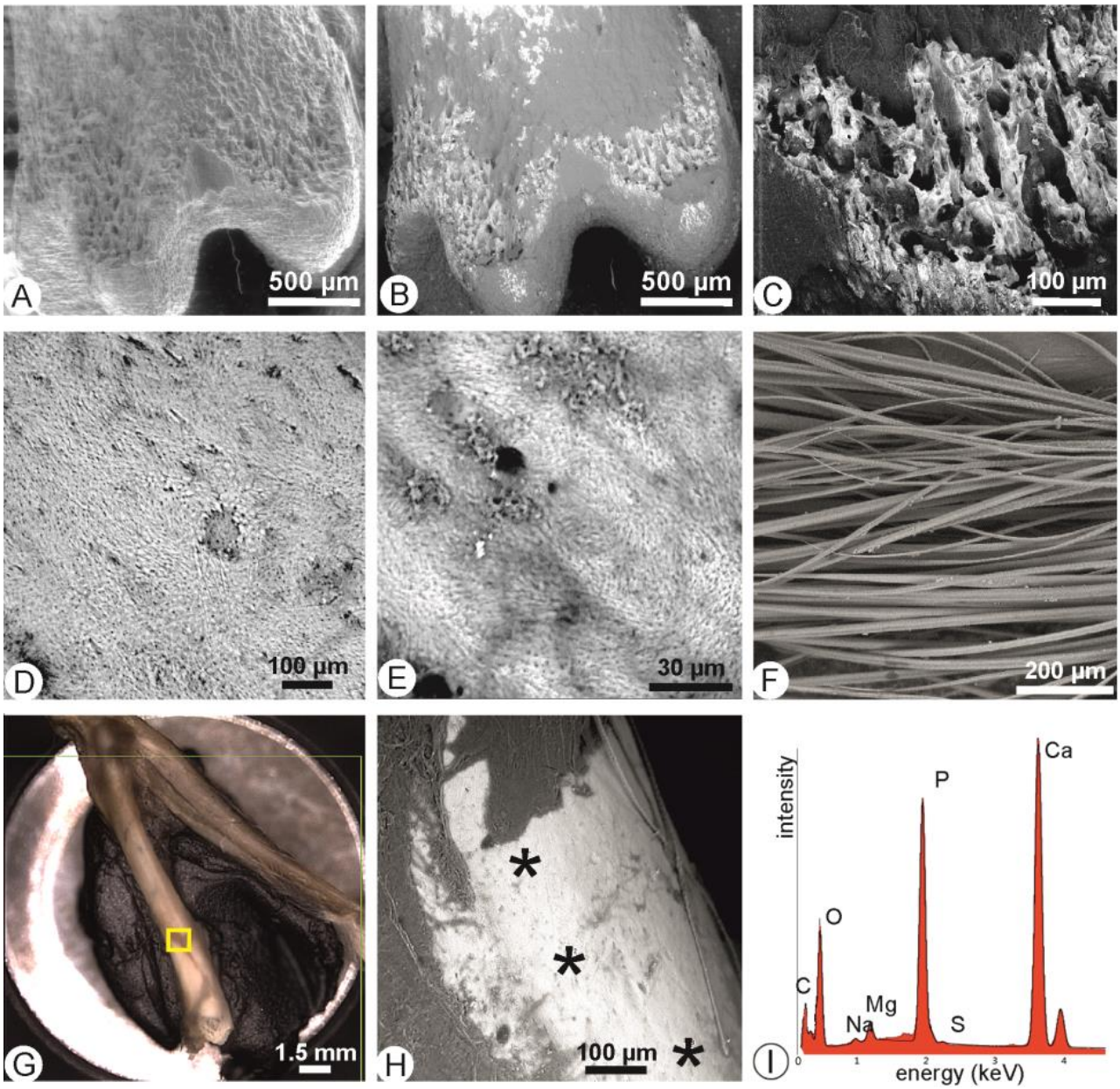

Figure 5. Lipase etching. (**A**,**B**). SE (**A**) and BSE (**B**) images of the extremity of a femur of *Apodemus* showing the presence of organic remains. (**C**). Cancellous structure rich in organic matrix; BSE image. (**D**–**E**). Haversian structure visible in clean zones of the scapula of *Apodemus*. (**F**). Hairs are not etched in the same sample. (**G**). Optical image showing clean pale yellow bone, and brown zones with flesh are brown. (**H**). Localization of electron microprobe spectra: stars (**I**). Spectra show that P and Ca are present as well as Na, Mg and S.

3.6. Bones Extracted from Tyto alba Pellets

Stereomicroscope observations show that the femur has light to moderate digestion according to Andrew's criteria [2] (Table S1). The porous structure of the cancellous bone is visible on the epiphyses and in some parts of the diaphysis (Figure 7A–D). Most flesh and hairs have been removed by the digestion process except in Figure 7K,L. There are holes of different sizes at the surface of the articular surface of a bone (Figure 7B,C) or at the diaphyseal surface (Figure 7H,J). This is also visible at higher magnification (Figure 7E). The bone surface of the diaphysis is not equally affected by digestion, and some patches of compact bone remain between holes (Figure 7F–G,L). Holes have various depths and some show a polished and rounded aspect (Figure 7H,I). Little cracks are observed on

the articular and diaphysis compact bone surfaces (Figure 7B,D,J) whose digestion or post-predation origin is not clear (weathering, desiccation, etc.).

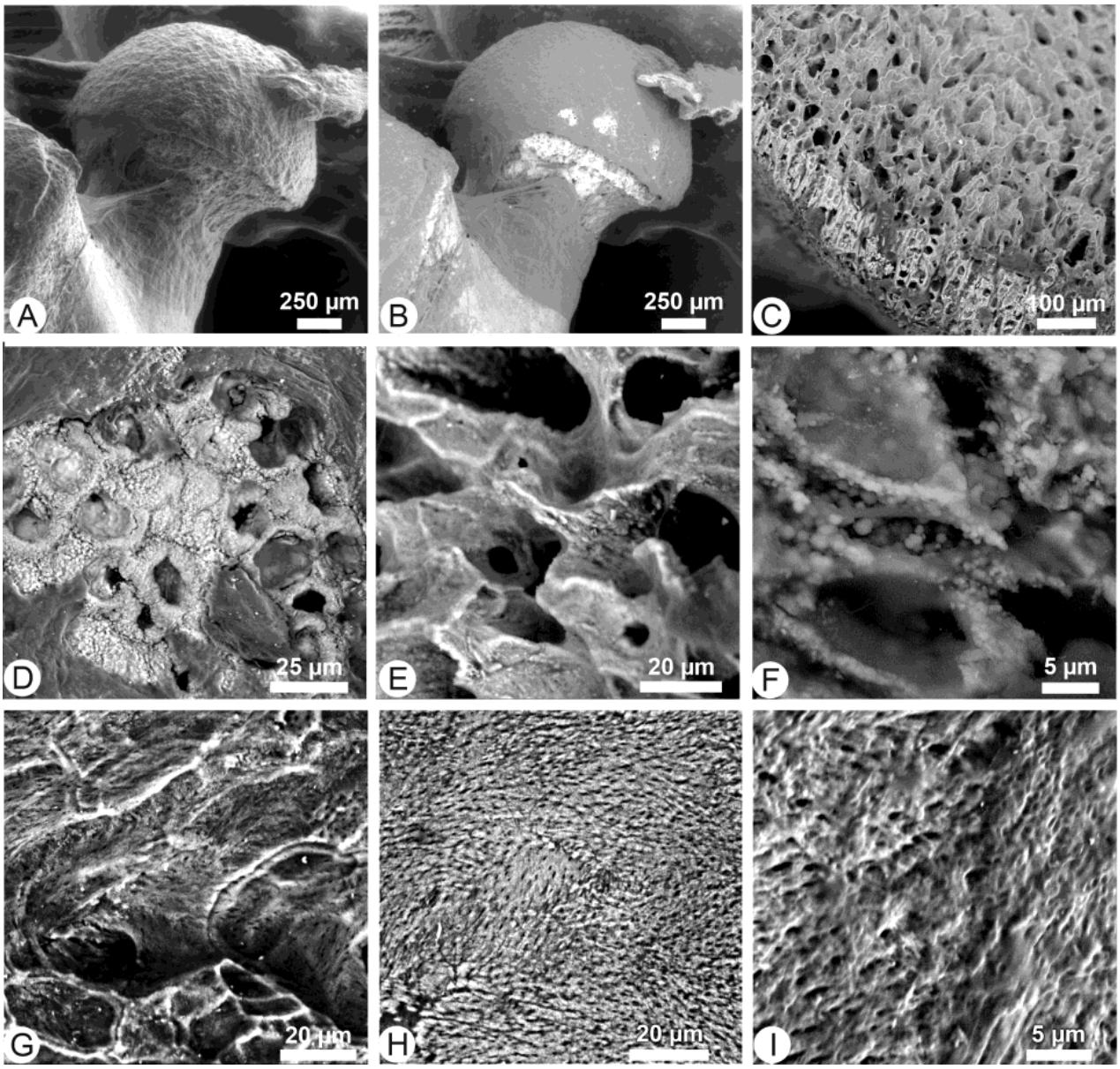

Figure 6. Tryspin and lipase etchings. (**A**,**B**). Irregular etching of the epiphysis of a femur of *Apodemus*; SE (**A**) and BSE (**B**) images. (**C**). Fractured tibia of *Apodemus*. (**D**). Irregular etching of the epiphysis of a femur of *Apodemus;* BSE image). (**E**,**F**). Cancellous zone of a tibia *Apodemus* showing small, rounded granules. (**G**–**I**). Bone resorption patterns in the same sample (**G**,**H**) and in the femur of *Mus musculus* (**I**).

3.7. Bones Extracted from Bubo bubo Pellets

Femurs extracted from the *Bubo bubo* pellets display digestion at both epiphyses and diaphyses (Figure 8). Observed under the stereomicroscope, these bones exhibit moderate and strong grades of digestion according to Andrews [7] (Table S1). The spongy structure of the epiphyses is visible, with large holes having irregular sizes (Figure 8A,B). The outer layer of the bone is digested in the diaphysis (Figure 8C). The enlarged cavities contain submicrometer spherules (Figure 8D,E), the nature and origin of which are not yet known. Some epiphysal regions are not so strongly etched (Figure 8F), but the structure is visible. The digestion process has not destroyed all hairs, and flesh remains visible both on the

epiphysis (Figure 8G) and diaphysis surfaces (Figure 8H). The surface of the diaphysis is visible, and the haversian structure is displayed (Figure 8I).

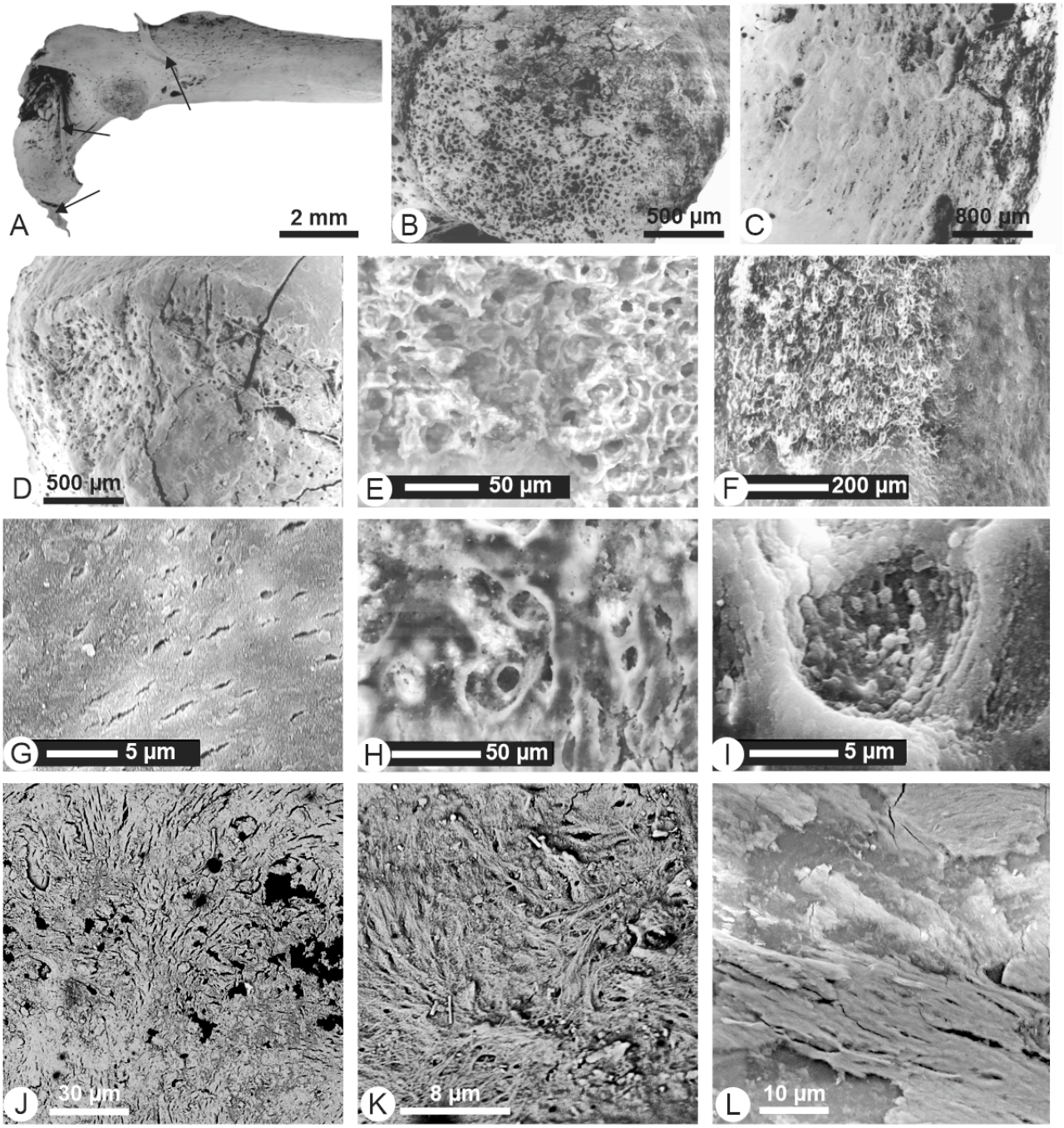

Figure 7. Rodent bones extracted from *Tyto alba* pellets from Mauritania. (**A**). Proximal articular zone of a digested femur displaying characteristic holes and cancellous bone exposed both on articular and diaphysis surfaces. Some hairs and muscle fibers are still sticking to the bone surface (arrows). (**B**). Detail of same femur with cancellous bone exposed, showing enlarged cavities typical of light digestion grade. (**C**). Detail showing the surface alteration due to digestion, notice the irregular surface with some smooth polished parts and sinuous outline following the underlying cancellous layer locally exposed. Some holes of various sizes correspond to enlarged natural cavities. On the right part of the picture one can see some relatively deep cracks following enlarged holes. (**D**). Detail

of the contact between articular surface and diaphysis of another femur with cancellous bone and some polishing due to light digestion. Cracks probably occurred after digestion and may be due to weathering action on pellets accumulated in a tropical climate. (**E**). Detail of the enlarged natural cavities at the articular zone of a moderately digested bone with typical structure of holes and their border with smooth surrounding zones. (**F**). Outer surface of a femur diaphysis showing a smooth zone on the right and a digested zone on the left. (**G**). Surface of the diaphysis of another femur displaying the cancellous structure and some polishing typical of digestion. (**H**). Etched diaphysis of another femur showing enlarged cavities separated by a smooth polished surface due to digestion. (**I**). Detail of a cupule on the diaphysis of a femur, showing a granular structure and some smooth borders typical of the enlarged cavities of digested bones. (**J**). Surface of the femur near the epiphysis displaying different sizes of cavities and enlarged ones separated by a polished surface. (**K**). Same bone, near the other extremity of the femur displaying a rougher, fibrous aspect and few signs of digestion like cavities of various diameter and smooth zones. (**L**). Etched surface of the diaphysis of another femur displaying some layers of differentially eroded fragments, with on the first plan probable cracking due to weathering superimposed to digestion.

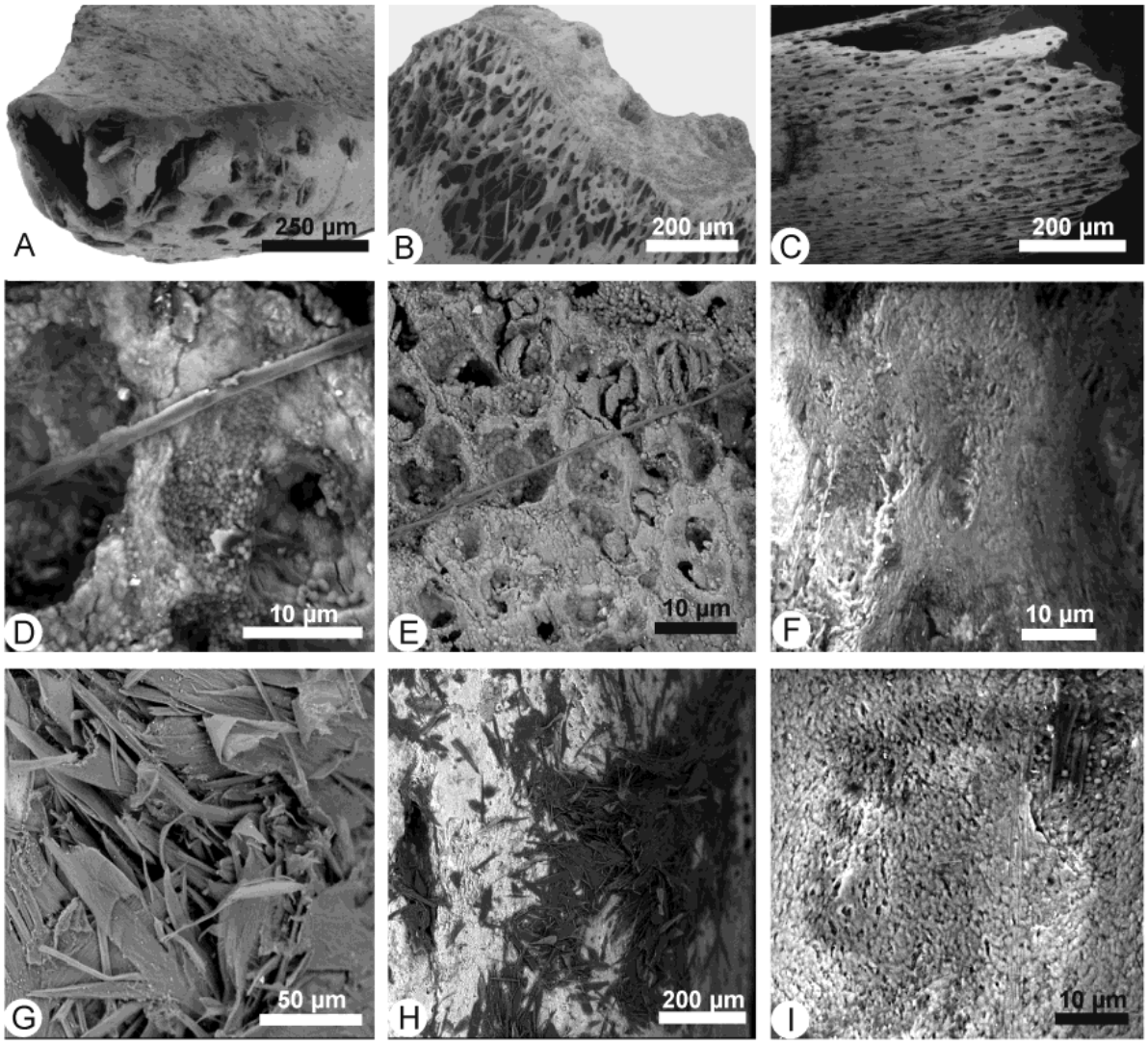

Figure 8. Murid rodent bones from *Bubo bubo* pellets. (**A**). Humerus distal epiphysis displaying a moderate stage of digestion with holes of different sizes and depth upon the articular zone; the compact

bone layer is removed on the diaphysis. (**B**). Articular zone of an undetermined bone with heavy digestion and removing of a large part of cancellous bone. (**C**). Compact layer removed and cancellous bone in a broken diaphysis of an undetermined bone. (**D**). Femur epiphysis showing enlarged cavities with granular structure and hair. (**E**). Same sample, showing the cancellous surface and enlarged cavities separated by smooth surfaces and covered of small granules of unknown origin. Rodent hair at the surface. (**F**). Epiphysis of a femur displaying cancellous bone and some enlarged cavities. (**G**). Outer surface of the same femur diaphysis showing remnants of muscle and hairs. (**H**). Same sample, the outer surface is only partially covered by the remnants of muscle. (**I**). Diaphysis of a femur showing the typical light digestion pattern with cancellous bone exposed and remains of hairs.

4. Discussion

These experiments have obvious limitations: only a few taxa were used, the samples are small, only a few skeletal elements were examined, and only some of the known or possible digestive compounds were tested. As we discuss the structural and compositional features of the samples, it is important to acknowledge that digestion is a complex physiological process, and our study was only able to begin addressing some of the factors contributing to bone surface modification.

4.1. Samples

Only four specimens from two rodent species were used in these experiments. They were young and adult individuals of the same rodent sub-family (Murinae). The number of individuals is low, but the structure of bones does not differ at this scale of observation. In addition, the composition of bones (bioapatite, collagen, osteopont) are similar in all species. Species-specific proteins, lipids, or sugars exist, but the most abundant organic component is collagen. Therefore, we assumed that the species-level differences in bone structure and composition were not large enough to be visible in the induced modifications.

4.2. Choice of Experimental Conditions

Previous etching experiments have investigated the effects of hydrochloric acid on teeth [18], and hydrochloric acid and enzymes on bone [31].

Genes related to the production of digestive enzymes such as lipases and proteases are dominant in carnivorous birds, whereas insectivorous birds have more abundant genes related to the production of chitinases [30]. Data on the pH and components of gastric juices of birds of prey are scarce. As for other predators, pH is acidic but shows large variations in a single animal. Only HCl is mentioned. Thus, we have used HCl solutions at pH 1 and 2.43 to follow preprandial gastric juice pH observations [32]. In barn owls, the pH range is between 2.5–5.0 [33].

Among the enzymes, amylase, chitinase, trypsin, chymotrypsin, carboxypeptidase, and pepsin were identified, but their proportion is not known and probably varies among taxa, and throughout the life span of a bird [33]. Trypsin, chymotrypsin, and pepsin are proteases that cleave proteins and peptide chains to form smaller peptides. Trypsin, commonly found in the digestive tracts of vertebrates, has an optimal activity at pH between 7.5 and 8, at about 37 °C. Pepsin has an optimal activity at pH 2 at about 37–42 °C, and is activated by HCl. Thus, it is difficult to deduce the individual role of pepsin and that of HCl, and we do not use pepsin. Lipase is involved in the hydrolysis of lipids, with an optimal activity at pH about 8, at 37 °C [34].

Chitin is a major component of arthropods and worms, and chitinase cuts the glycosidic bonds. Insects are common in regurgitation pellets, but bone does not contain chitin, so chitinase was not used in these experiments.

During normal digestion, HCl secreted by the proventriculus has two actions: etching of soft and mineralized tissues, and activation of the pepsinogen, so that a first step of enzymatic hydrolysis is completed at this stage. pH varies before and after the prandial phase [31], but the evolution of the composition of the gastric juices and the concentrations of enzymes are known for only some predators [35,36]. Thus, in this preliminary study,

enzymes and acids have not been used together, and only fixed concentrations have been tested. Similarly, bacteria are not taken into account, despite the fact that they are known to occur in digestive tracts [35].

4.3. Physical Parameters

The temperature of the digestion process is the best-known parameter and is easy to reproduce. Another important parameter is the quantity of gastric juice present during digestion. Prior studies have indicated only that gastric secretion "is not profuse" [37]. Duke et al. [33] mentioned that basal gastric juice samples were difficult to obtain and varied between the species of raptors studied. The ratio between liquid and bones we used was empirically fixed and is probably different from that found in the owl stomach. The presence of liquid in our experiments may have induced some dissolution. It is worth noting that Duke et al. [33] had to dilute their samples of gastric juices to be able to measure proteolytic activity. Another concern is the skin, hairs, and flesh in the experiments; only some remnants were preserved before the experimental digestion, so that the surface of the bones was not in direct contact with the solution. Nevertheless, bones were fully decalcified using the acidic hydrolysis as shown by EDS spectra. Agitation-motility during in vivo digestion exists, but how it influences the preservation of bones is not yet understood.

In this experiment, enzymes were dissolved in a TRIS buffer. This buffer is a water solution, inducing some dissolution of the soft and hard parts of the samples, but natural digestion also involves liquid.

4.4. In Vitro Digestion Effects

The gastric juices of birds of prey contain enzymes (chymotrypsin, amylase, etc.) [33,36] not used in this experiment. Amylase is mainly present in saliva in mammals, and it hydrolyses starch into sugars. Its optimal activity is at pH 6.7–7. Carboxypeptidase hydrolyses proteins; its optimal pH varies between 7 and 9. Here, we have selected the most common enzymes for proteins and lipids, and HCl for the soft and hard tissues.

All the enzymes used in this study were efficient in etching the bones. The most visible difference is the degree of alteration. The effects of lipase are the least visible. Is this result due to the concentration of lipase in the experiment or to the quantity of lipids in the bone? Additional experiments are necessary to address this question. Samples in lipase and trypsin were the most digested: the surface of the bone is "clean", visible, with the haversian structure and the alveolar zone, the empty channels of the blood vessels, etc. Bones digested in trypsin were more similar to bones digested by owls than those etched with lipase. Resorption lacunae do not seem to be enlarged by the etchings. Nevertheless, osteoclasts implied in the turnover of the bone tissue were removed by the enzymatic etchings [38–41].

Although detailed chemical analyses have not been performed on these samples, EDS spectra show that chemical modifications exist. Previous analyses have shown that every predator imparts its own chemical signature on bones and teeth [42,43]. These particularities depend upon the unique composition of the gastric juices for a given raptor.

Soft tissues were still present after the cleaning processes, meaning that the results differ from those described by Fernandez-Jalvo et al. [17]. These authors have used bones and teeth extracted from regurgitated pellets for in vitro digestion and abrasion. These bones are devoid of flesh, skin, and hair, so they are probably more sensitive to the acid and enzymes. Moreover, the bones used for this experiment are weakened because they are already digested [21]. Detailed structural observations were not available for this work. Another experimental study of the influence of acidic environments on bones was recently conducted [44]. In that study, bones were defleshed and submitted to sulfuric acid for several days. Thus, a detailed comparison with these data is not complete.

4.5. Comparison of In Vitro and In Vivo Alterations

When comparing the results of this experiment with the pattern observed on digested bones, we can observe a difference in the intensity of the digestion between *Tyto alba* and *Bubo bubo* which confirms previous studies [7,8,28,42,43]. Nevertheless, some similarities with in vitro digestion are visible. On the epiphyses, dissolution holes seem more prominent (larger and deeper) in *Bubo bubo* than on *Tyto alba*. The cancellous bone surface looks more rugose and with higher relief (less polished surfaces) in *T. alba*. A similar distinction was described by Andrews [8] (Table S1) who classified *T. alba* in category 1 of digestion (low modification) and *B. bubo* in category 3 (moderate digestion).

One similarity concerns the remains of little hairs and flesh on in vitro and in vivo digested bones. Some similarities of the surface alterations between bones submitted to trypsin hydrolyses, for instance Figures 4D and 7B,D (*T. alba*) or Figures 4F and 8C (*B. bubo*), are also visible. With the lipase only, no similar results are observed for both predators. However, when trypsin and lipase are combined, the results look identical to some of the figures resulting from predation. In fact, Figure 6A–C,I are reminiscent of Figure 8A,I (*B. bubo*) or Figure 7B,E *(T. alba*). Figure 6F is similar to Figure 8I (*B. bubo)* and Figure 6G to Figure 7C (*T. alba*). At a higher magnification, Figures 6G and 4G are reminiscent of Figure 7H,I (*T. alba*) and Figure 8E (*B. bubo*). In all cases, hairs are resistant to in vitro and in vivo alterations.

Clearly, we obtained greater similarity in the experimental treatments with owl pellet digestion in the etching of bone surface using trypsin and trypsin + lipase than with HCl or lipase only. This corroborates a previous experiment that demonstrated that HCl alone is insufficient for digestion, and it must be combined with enzymatic attack [31,33].

Previous experiments using pronase resulted in strong etching of bone surfaces similar to that induced by diurnal birds of prey. Trypsin and lipase resulted in patterns similar to nocturnal birds of prey, which have low to medium intensity of digestion. Thus, bones and teeth are more abundant in pellets from nocturnal birds [33,45]. *Tyto alba* and *Bubo bubo* are Strigiformes nocturnal birds of prey, and their digestive tract has no crop (a storage organ).

5. Conclusions

With simple experiments on a few long bones, we tested the action of two enzymes on bone digestion and found patterns of bone modification similar to those seen in pellets. These results open a promising field of experimentation to identify the characteristic signature of raptor digestion on bone surfaces and to understand the effect of digestion and its influence on fossilization. This preliminary neotaphonomic work must be extended by mixing various enzymes, by varying the pH over time, or by replicating the experiments using different long bones and teeth. We compared our results with only two predators, but there are many species that are known to occur today or are thought to be responsible from some fossil accumulations. The modern reference baseline is still under construction, and we are far from knowing all the aspects of digestion processes on bone and teeth. A deeper knowledge of this important step of pre-diagenetical alteration of small mammal bone is important for interpreting archaeological and palaeontological assemblages. Accounting for digestive modifications should precede further paleoenvironmental analysis. Understanding the effects of different taphonomic agents will improve our understanding of fossilization patterns and processes.

Supplementary Materials: The following supporting information can be downloaded at: https://www.mdpi.com/article/10.3390/min13010124/s1, Figure S1: Summary of birds digestive tracts and enzymes involved into digestion [45]; Figure S2: Anatomical position of rodent bones submitted in this work to experimental acidic and enzymatic digestions.; Figure S3: Aspect of mouse unetched bones; Figure S4:Graph and SEM pictures of the long bone microstructure; Table S1: Predators categories and induced dammages.

Author Contributions: Conceptualization, C.D. and Y.D.; investigation, Y.D. and C.D.; writing—original draft preparation—review and editing, Y.D., D.N.R. and C.D.; funding acquisition, C.D. and Y.D.; All authors have read and agreed to the published version of the manuscript.

Funding: Partial funding was obtained for this work through the GDR 3561 CNRS Taphen (Dr J.P. Brugal dir.).

Data Availability Statement: Not applicable.

Acknowledgments: The authors thank V. Nicolas (UMR 7205) for providing one wood mice from France.

Conflicts of Interest: The authors declare no conflict of interest.

References

1. Efremov, I.A. Taphonomy: A new branch of paleontology. *Pan-Amer. Geol.* **1940**, *74*, 81–93.
2. Fernandez-Jalvo, Y.; Andrews, P.; Denys, C.; Sese, C.; Stoetzel, E.; Marin Monfort, D.; Pequero, D. Taphonomy for taxonomists, implications in small mammal studies. *Quarter. Sci. Rev.* **2016**, *139*, 138–157. [CrossRef]
3. Klaphake, E.; Clancy, J. Raptor gastroenterology. *Vet. Clin. Exotic Animal* **2005**, *8*, 307–327. [CrossRef] [PubMed]
4. Weissbrod, L.; Dayan, T.; Kaufman, D.; Weinstein-Evron, M. Micromammal taphonomy of el-Wad Terrace, Mount Carmel, Israel: Distinguishing cultural from natural depositional agents in the Late Natufian. *J. Archaeol. Sci.* **2005**, *32*, 1–17. [CrossRef]
5. Reed, D.N. Taphonomic implications of roosting behavior and trophic habits in two species of African owl. *J. Archaeol. Sci.* **2005**, *32*, 1669–1676. [CrossRef]
6. Fernandez-Jalvo, Y.; Avery, D.M. Pleistocene micromammals and their predators at Wondevewerk Cave, South Africa. *Afr. Arch. Rev.* **2015**, *32*, 751–791. [CrossRef]
7. Fernandez-Jalvo, Y.; Andrews, P. *Atlas of Taphonomic Identifications: 1001+ Images of Fossil and Recent Mammal Bone Modification*; Springer: Dordrecht, The Netherlands, 2016; 359p.
8. Andrews, P. *Owls, Caves and Fossils*; Natural History Museum Publications: London, UK, 1990.
9. Barbosa, B.B.; Barauna, A.C.G.; Domingues, S.F.S. Birds of prey pellet analysis: Morphometry and consumption interval of captive Accipitridae species. *Cienca Animal* **2021**, *31*, 30–37.
10. Bochenski, Z.M.; Tomek, T. Preservation of bird bones: Erosion *versus* digestion by owls. *Intern. J. Osteoarch.* **1997**, *7*, 372–387. [CrossRef]
11. Fernandez-Jalvo, Y.; Andrews, P. Small Mammals taphonomy of Grand Dolina, Atapuerca (Burgos), Spain. *J. Archaeol. Sci.* **1992**, *19*, 407–428. [CrossRef]
12. Rensberger, J.M.; Krentz, H.B. Microscopic effects of predator digestion on the surfaces of bones and teeth. *Scanning Microsc.* **1988**, *2*, 30.
13. Comay, O.; Dayan, T. Taphonomic signatures of owls: New insights into micromammal assemblages. *Palaeogeogr. Palaeoclim. Palaeoecol.* **2018**, *492*, 81–91. [CrossRef]
14. Simmons, R.E.; Avery, D.M.; Avery, G. Biases in diets determined from pellets and remains: Correction factors for a mammal and bird-eating raptor. *J. Raptor Res.* **1991**, *25*, 63–67.
15. Marchesi, L.; Pedrini, P.; Sergio, F. Biases associated with diet study methods in the European eagle—Owl. *J. Raptor Res.* **2002**, *36*, 11–16.
16. Denys, C. Des référentiels en taphonomie des petits vertébrés: Bilan et perspectives. In *Taphonomie des Petits Vertébrés: Référentiels et Transferts Aux Fossiles*; Laroulandie, V., Mallye, J.B., Denys, C., Eds.; Series 2269; British Archaeological Reports Oxford Ltd.: Oxford, UK, 2011; pp. 7–22.
17. Fernandez-Jalvo, Y.; Andrews, P.; Sevilla, P.; Requejo, V. Digestion *versus* abrasion features in rodent bones. *Lethaia* **2014**, *47*, 323–336. [CrossRef]
18. Weber, K.; Winkler, D.E.; Schulz-Kornas, E.; Kaiser, Y.M.; Tütken, T. The good, the bad and the ugly—A visual guide for common post-mortem wear patterns in vertebrate teeth. *Palaeogeogr. Palaeoclim. Palaeoecol.* **2021**, *578*, 110577. [CrossRef]
19. Kusmer, K.D. Taphonomy of owl pellet deposition. *J. Paleont.* **1990**, *64*, 629–637. [CrossRef]
20. Yalden, D.W.; Yalden, P.E. An experimental investigation of examining Kestrel diet by pellet analysis. *Bird Study* **1985**, *32*, 50–55. [CrossRef]
21. Denys, C. Taphonomie des sites à petits vertébrés, importance de la digestion et des altérations post-prédation. In *Manuel de Taphonomie*; Denys, C., Pathou-Mathis, M., Eds.; Errance Editions: Paris, France, 2014; pp. 101–122.
22. Denys, C. Accumulations de rapaces nocturnes et diurnes. *TaphonomieS. Paris: Éditions Des Arch. Contemp.* **2017**, 347–367.
23. Shipman, P. Applications of scanning electron microscopy to taphonomic problems. *Ann. N. Y. Acad. Sci.* **1981**, *376*, 357–385. [CrossRef]
24. Cummings, J.H.; Duke, G.E.; Jegers, A.A. Corrosion of bone by solutions simulating raptor gastric juices. *Raptor Res.* **1976**, *10*, 55–57.
25. Terry, R.C.; Laney, J.A.; Hay-Roe, S.H. Quantifying the digestive fingerprints of predators on the bones of their preys using scanning electron microscopy. *Palaios* **2018**, *33*, 487–497. [CrossRef]

26. Bruderer, C.; Denys, C. Inventaire taxonomique et taphonomique d'un assemblage de pelotes d'un site de nidification de *T. alba* de Mauritanie. *Bonner Zool. Beit.* **1999**, *48*, 245–257.
27. Dodson, P.; Wexlar, D. Taphonomic investigations of owl pellets. *Paleobiology* **1979**, *5*, 275–284. [CrossRef]
28. Denys, C.; Dauphin, Y.; Rzebik-Kowalska, B.; Kowalski, K. Taphonomic study of Algerian owl pellet assemblages and differential preservation of some rodents: Palaeontological implications. *Acta Zool. Crac.* **1996**, *39*, 103–116.
29. Lopez, J.M. Actualistic taphonomy of barn owl pellet derived small mammal bone accumulations in arid environment of South America. *J. Quater. Sci.* **2020**, *35*, 1057–1069. [CrossRef]
30. Boyde, A.; Jones, S.J. Back-scattered electron imaging of skeletal tissues. *Metab. Bone Dis. Rel. Res.* **1983**, *5*, 145–150. [CrossRef] [PubMed]
31. Denys, C.; Fernandez-Jalvo, Y.; Dauphin, Y. Experimental taphonomy: Preliminary results of the digestion of micromammal bones in the laboratory. *C. R Acad. Sci. Paris* **1995**, *321*, 803–809.
32. Chen, Y.-H.; Zhao, H. Evolution of digestive enzymes and dietary diversification in birds. *PeerJ* **2019**, *46*, 73–82. [CrossRef]
33. Duke, G.E.; Jegers, A.A.; Loff, G.; Evanson, O.A. Gastric digestion in some raptors. *Comp. Biochem. Physiol.* **1975**, *50A*, 649–656. [CrossRef]
34. Ben Bacha, A.; Frikha, F.; Djemal, I.; Fendri, A.; Miled, N.; Gargouri, Y.; Medjoub, H. Biochemical and structural comparative study between bird and mammal pancreatic colipases. *J. Lipid Res.* **2006**, *47*, 2701–2711. [CrossRef]
35. Daneel, A. Dietary Modulation of Intestinal Fermentation in Raptors. Master's Thesis, Faculty of Veterinary Medicine, Ghent University, Ghent, Belgium, 2018.
36. Leprince, P.; Dandrifosse, G.; Schoffeniels, E. The digestive enzymes and acidity of the pellets regurgitated by raptors. *Biochem. System. Ecol.* **1979**, *7*, 223–227. [CrossRef]
37. Reed, C.I.; Reed, B.P. The mechanism of pellet formation in the Great Horned Owl (*Bubo virginianus*). *Science* **1928**, *68*, 359–360. [CrossRef]
38. Boyde, A.; Hobdell, M.H. Scanning electron microscopy of lamellar bone. *Z. Zellforsch.* **1969**, *93*, 213–231. [CrossRef] [PubMed]
39. Chambers, T.J.; Revell, P.A.; Fuller, K.; Athanasou, N.A. Resorption of bone by isolated rabbit osteoclasts. *J. Cell Sci.* **1984**, *66*, 383–399. [CrossRef] [PubMed]
40. Gentzsch, C.; Delling, G.; Kaiser, E. Microstructural classification of resorption lacunae and perforations in human proximal femora. *Calcif. Tissue Int.* **2003**, *72*, 698–709. [CrossRef]
41. Hefti, T.; Frischherz, M.; Spencer, N.D.; Hall, H.; Schlottig, F. A comparison of osteoclast resorption pits on bone with titanium and zirconia surfaces. *Biomaterials* **2010**, *31*, 7321–7331. [CrossRef]
42. Dauphin, Y.; Denys, C.; Denis, A. Les mécanismes de formation des gisements de microvertébrés: Modifications de la composition chimique des os et dents de rongeurs issus de pelotes de régurgitation de rapaces. *C. R. Acad. Sci. Paris* **1988**, *307*, 603–608.
43. Dauphin, Y.; Denys, C.; Denis, A. 1989. Les mécanismes de formation des gisements de microvertébrés. 2- Composition chimique élémentaire des os et dents de rongeurs provenant de pelotes de régurgitation. *Bull. Mus. Natl. Hist. Nat.* **1989**, *11*, 253–269.
44. High, K.; Milner, N.; Panter, I.; Penkman, K.E.H. Apatite for destruction; investigating bone degradation due to high acidity at Star Carr. *J. Arch. Sci.* **2015**, *50*, 159–168. [CrossRef]
45. Duke, G.E.; Evanson, O.A.; Jegers, A. Meal to pellet intervals in 14 species of captive raptors. *Comp. Biochem Physiol.* **1976**, *53A*, 1–6. [CrossRef]